J. Fluid Mech. (1972), *vol.* 55, *part* 1, *pp.* 31–48
Printed in Great Britain

The vortex street in the wake of a vibrating cylinder

By OWEN M. GRIFFIN AND CHARLES W. VOTAW
Naval Research Laboratory, Washington, D.C. 20390

(Received 20 September 1971)

The von Kármán vortex streets formed in the wakes of vibrating smooth cylinders and cables were studied using a hot-wire anemometer and flow visualization by fog injection in a wind tunnel. All the experiments took place in the flow regime where the vibration and vortex-shedding frequencies lock together, or synchronize, to control the formation of the wake. Since the flow in the vortex formation region is fundamental to further understanding of the interaction between a vibrating bluff obstacle and its wake, detailed measurements were made of the formation-region flow for Reynolds numbers between 120 and 350. The formation-region length is shown to be a fundamental parameter for the wake, and is dependent on a shedding parameter St^* related to the naturally occurring Strouhal number for the von Kármán street. The effects of vibration amplitude and frequency on the mean and fluctuating velocity fields in the wake become apparent when the downstream displacement is scaled with the formation length. The von Kármán vortex street behind a vibrating cylinder is divided into three predominant flow regimes: the formation, stable and unstable regions. Fundamental differences exist in the vortex streets generated behind stationary and vibrating cylinders, but many classical characteristics, including the manner of vortex breakdown in the unstable region, are shared by the two systems.

1. Introduction

It is a well-known phenomenon of fluid mechanics that the periodic shedding of vortices due to the crossflow past a cable or other bluff obstacle can excite the body into resonant transverse vibrations when the vortex frequencies and the body frequency are sufficiently close to one another. There is also a range of forced frequencies near the Strouhal frequency of vortex shedding where the vibration and vortex frequencies lock together, or synchronize, and control the shedding process. This synchronization phenomenon is of both practical and fundamental importance, and the summary of a recent Euromech Colloquium by Mair & Maull (1971) stresses the need for controlled experiments to investigate further the effects of vibration amplitude and frequency on this synchronization, or frequency-locking, characteristic of wake flows. Tube bundle heat exchangers for nuclear power generation and underwater towing and instrumentation systems are three areas where investigations of cable strumming and other resonant flow-excited vibration phenomena are important for the improvement of design criteria and for the extension of the present state of our knowledge.

The real origin of vortex-excited vibrations lies in the fundamental mechanism of the vortex formation and shedding process. With this in mind, the writers have recently undertaken a study of the frequency-locking phenomenon and its relation to the vortex-excited resonance of bluff bodies. It is our purpose in the present paper to examine, using hot-wire and flow-visualization results, the changes in the formation and development of the von Kármán vortex street that accompany the frequency locking for Reynolds numbers up to 350. Measurements have been made of the vortex formation, the accompanying changes in the mean and fluctuating velocity fields, and the vortex wake geometry.

2. Related investigations

There is a considerable body of knowledge related to the resonant response characteristics of freely vibrating cylinders, but few investigations have been made of the interaction between a cylinder and its wake. The work of Ferguson & Parkinson (1967) concerned with fluctuating pressure and phase measurements at the cylinder and in the wake for Reynolds numbers near $Re = 10^4$ is of importance, as are the results of Mei & Currie (1969) of hot-wire measurements of changes in the separation region that accompany different combinations of frequency and amplitude. More recently, Griffin (1972) has investigated the vortex-formation region and fluctuating velocity field near a resonantly vibrating cylinder for Reynolds numbers between 550 and 900, and has compared the results with those obtained in the wake of a cylinder that was forced to vibrate under the same conditions. Early cylinder force measurements in the frequency-locked flow regime were made by Bishop & Hassan (1964) and later measurements by Toebes & Ramamurthy (1967) for Reynolds numbers near 10^4–10^5. Recently Toebes (1968) has measured velocity fluctuations, flow correlation and base pressure near a forced vibrating cylinder and made an extensive survey of related work available at that time.

Roshko (1954*a*, *b*) and Bloor (1964) have shown that the lower Reynolds number range of vortex shedding behind a stationary cylinder is divided into two parts. The stable range $50 < Re < 150$–200 is characterized by vortices that remain laminar for many cylinder diameters downstream, and the transition range 150–$200 < Re < 300$–400 is marked by an intermittent type of flow with the laminar vortices progressively deteriorating through low frequency modulations and irregularities. Berger (1964, 1967) first observed that transverse vibrations at, and near, the natural vortex-shedding (Strouhal) frequency not only exhibit frequency locking, but also delay the initiation of turbulence and extend the stable vortex-shedding range to $Re \sim 300$–400. A flow-visualization study of the vortex wake geometry was made by Koopmann (1967), who also showed that the frequency-locking regime encompassed a range of ± 25–$30\,\%$ of the natural vortex-shedding frequency. Both Koopmann (1967) and Griffin (1971) have shown that the wake is essentially two-dimensional at vibration amplitudes above $10\,\%$ of a cylinder diameter for Reynolds numbers up to 300–400. Griffin also observed that the wake of the forced vibrating cylinder for frequency-locked conditions can be divided into the three classical downstream flow regimes of the

von Kármán street: the formation, stable and unstable regions. These regions had been observed by Schaefer & Eskinazi (1959) at Reynolds numbers below 120 for the stationary cylinder. The unstable region has been observed by Zdravkovich (1967, 1968) in the wakes of single cylinders and rod bundles and by Taneda (1955) for the single cylinder. Durgin & Karlsson (1971) have investigated vortex-street breakdown and have observed a flow regime that closely resembles the unstable region mentioned above.

3. Experimental apparatus and methods

The experiments reported in this paper were performed in an open jet wind tunnel equipped with a 75×75 mm exit and a 20:1 contraction section. Disa anemometers (model 55D01) and low interference hot-wire probes (model 55F01) were used for the flow measurements. The hot-wire output was carefully linearized in the speed range 0·25–2·5 m/s with a Disa linearizer (model 55D01), so that quantitative measurements of the mean and the large fluctuating velocities encountered in the range of the experiments could be interpreted with confidence. Smooth circular cylinders, 2·4 and 3·2 mm in diameter, were used in the hot-wire experiments and were mounted in a vibration isolated shaker at the exit jet of the tunnel. The wind tunnel and its supporting equipment have been described in detail previously (Griffin 1971, 1972).

Flow studies were conducted in the wind tunnel using a fog of minute oil droplets as the indicator. The contraction section of the tunnel was fitted with a slender airfoil section that spanned the contraction and had a slotted trailing edge and a splitter plate for the injection of the aerosol into the tunnel. Two hot wires were placed in the exit section of the tunnel, one outside the airfoil wake and the other downstream of the splitter plate, so that the indicator bleed rate could be adjusted to correct the wake defect. In this way a uniform velocity profile containing a sheet of indicator was obtained at the tunnel exit for the flow-visualization experiments. The flow indicator was generated by blowing compressed air through a container of di-(2-ethylhexyl)phtalate ($C_{24}H_{38}O_4$), or 'DOP', into a stagnation flow in a stripping mechanism to accumulate the large particles and to allow the small particles to pass into the injector mechanism. The remaining particles of DOP that were finally bled through the slotted airfoil had a size distribution approximately centred on 1 μm. The result was a laminar sheet of minute oil droplets and air that furnished a suitable indicator for wind-tunnel studies.

The co-ordinate system to which reference is made in the following sections is shown in figure 1. The origin is at the stationary cylinder centre with displacements in the flow direction denoted by x and those perpendicular to the flow direction denoted by y. The cylinder of diameter d_c was sinusoidally vibrated in a plane normal to the mean free-stream flow direction. The cylinder's amplitude of motion (peak-to-peak) is denoted by a, the cylinder frequency by f, and the natural vortex-shedding frequency for the stationary cylinder by f_n. Since all data were recorded in the frequency-locked regime, the cylinder and shedding frequencies are equal. This flow regime is illustrated in figure 2 for Reynolds

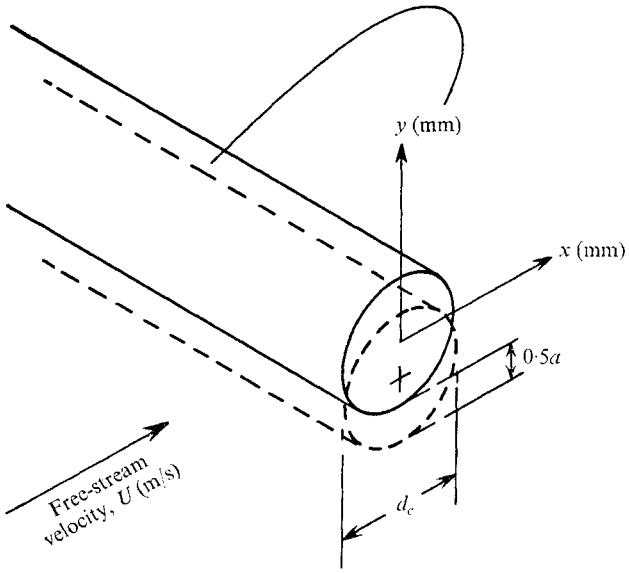

FIGURE 1. Cylinder and co-ordinate system.

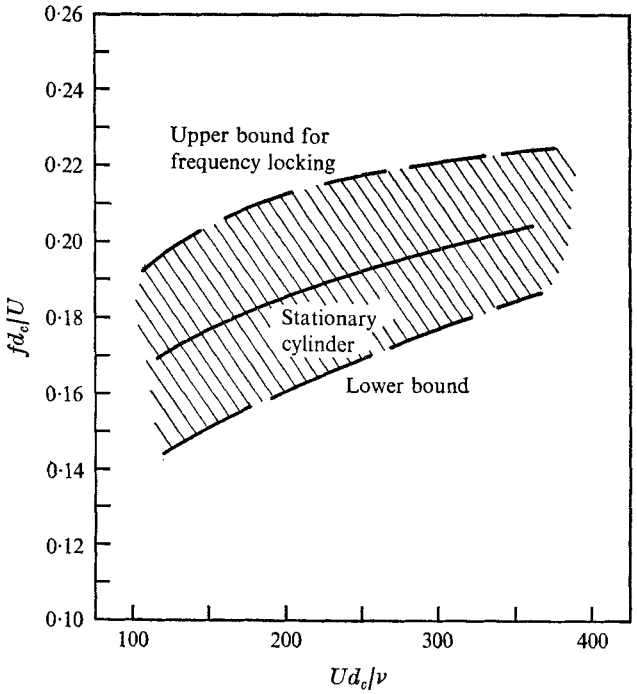

FIGURE 2. Representative bounds for the regime of frequency locking at Reynolds numbers between 120 and 350. The upper and lower bounds are from Koopmann (1967), for a cylinder amplitude of 0·2 diameter.

numbers between 120 and 350. The fluctuating velocity is denoted by u and represents the r.m.s. value measured at the hot-wire probe, the free-stream velocity is represented by U and the mean velocity by $\hat{U}(y)$. The Reynolds number (Ud_c/ν) is based on the mean free-stream velocity U, cylinder diameter d_c and kinematic viscosity ν. The Strouhal number St_n for natural shedding frequency f_n is defined as $f_n d_c/U$.

4. The formation and stable regions of the wake

The importance of the region of the wake where vortices are formed behind a bluff body has long been recognized, and answers as to the origin of vortex-excited vibrations lie in further knowledge of this formation and shedding process. Several physical cirteria have been defined for determining the initial position of a fully formed vortex and among them are the following.

(i) The minimum mean pressure on the wake axis, $y = 0$ (Roshko 1954*b*).

(ii) The maximum velocity fluctuation at the second harmonic of the shedding frequency, on the wake axis (Bloor & Gerrard 1966).

(iii) The minimum transverse spacing, close to the body, of the regions of maximum vortex velocity fluctuation (Schaefer & Eskinazi 1959; Bearman 1965).

Each of these three criteria yields essentially the same value for the formation length l_F, and can be measured with a pressure or hot-wire probe. The end of the formation region as indicated by the second of these criteria was measured in our experiments for several Reynolds numbers up to 350 and for conditions under which the vibration and vortex-shedding frequencies were locked together. The results are plotted in figure 3 as a function of the vortex-shedding parameter St^* defined by

$$St^* = (f/f_n)(1 + a/d_c)\, St_n,$$

and thus based on the amplitude a and frequency f of the vibrations. The wake width d_F is defined as the transverse distance between the maxima of the off-wake velocity fluctuations at formation, and the data cover a range of cylinder amplitudes from zero (stationary cylinder) up to half a diameter. The vibration frequencies were within $\pm 15\,\%$ of the Strouhal frequency at each Reynolds number, and individual values plotted have been tabulated in a report of related work (Griffin 1971).

The formation length decreases systematically with increased amplitude of cylinder vibration, while the effects of frequency changes are twofold. When the cylinder vibration frequency is decreased to a value less than the Strouhal frequency the distance to formation is increased. The flow in the formation region is related to that in the physical model recently postulated by Gerrard (1966) for the near wake of a stationary cylinder. A growing vortex is fed by circulation from the separated shear layer until it becomes strong enough to roll up and draw the opposing shear layer across the wake. This vorticity of opposite sign then cuts off further circulation to the growing vortex, which is then shed and begins to move downstream. The growing vortex behind the vibrating cylinder rolls up more quickly, draws the opposing shear layer across the wake and is

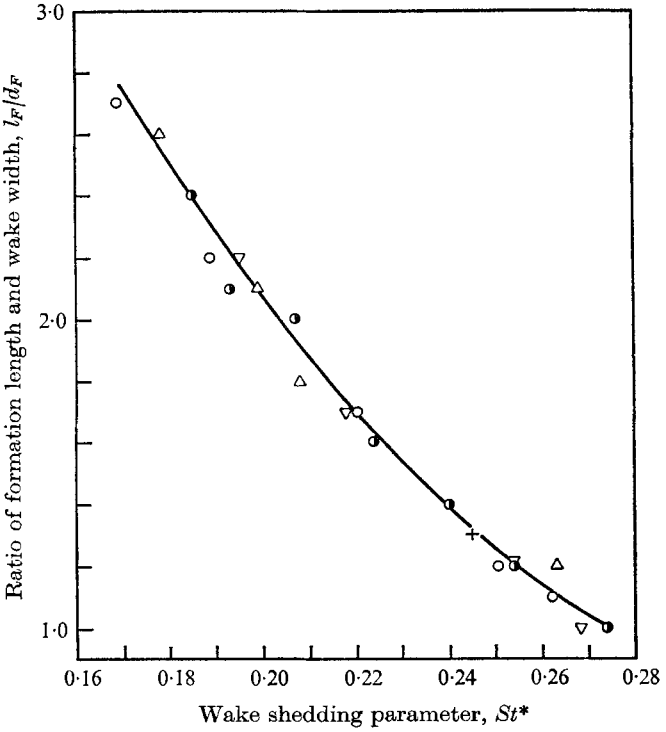

FIGURE 3. Ratio of formation length l_F and wake width d_F as a function of the shedding parameter St^*, for Reynolds number between 120 and 350. Reynolds number: ○, 120; △, 144; ◑, 200; ▽, 280; +, 350.

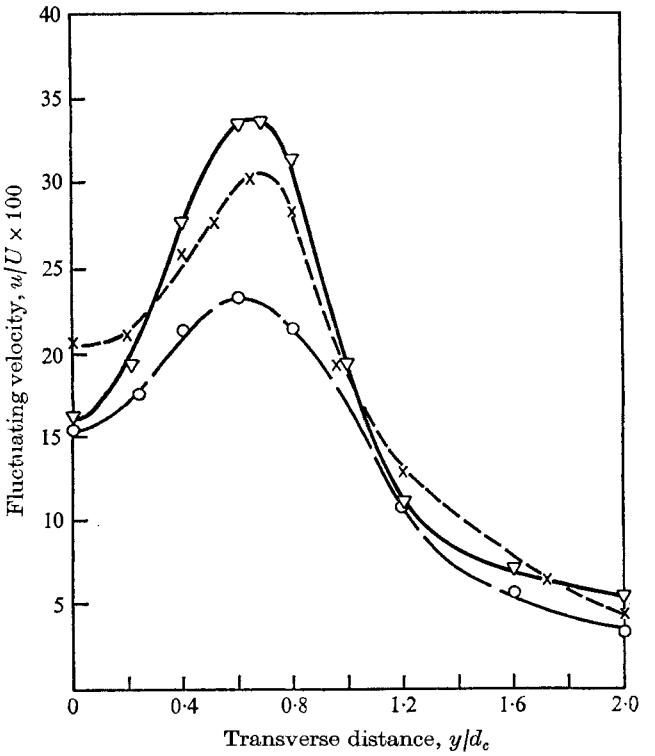

FIGURE 4. Root-mean-square velocity fluctuations at the end of the vortex-formation region for Re = 144. Frequency ratio f/f_n: — —, 0·90; – – × – –, 1·10. Amplitude a/d_c = 0·3 (both cases). —○—, stationary cylinder.

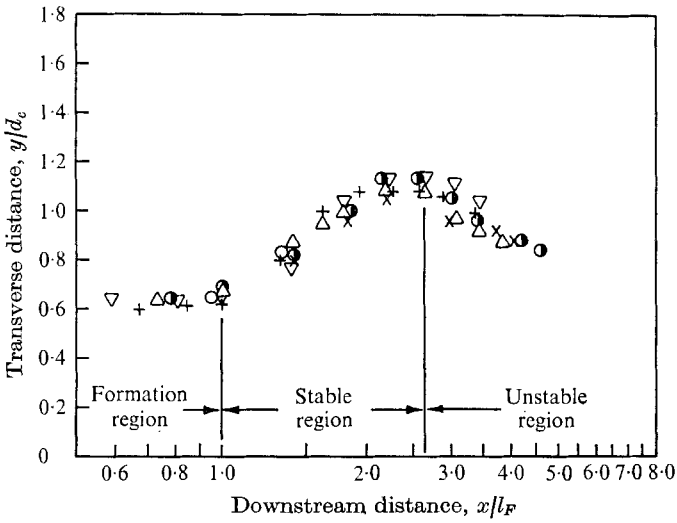

FIGURE 5. Distribution of the regions of maximum velocity fluctuation as a function of the scaled downstream distance x/l_F, at a Reynolds number of 144.

	○	+	△	◑	▽	×
St^*	0·178	1·99	0·231	0·263	0·208	0·254
f/f_n	1·00	1·00	1·00	1·00	0·90	1·10
a/d_c	0	0·12	0·30	0·48	0·30	0·30

shed at a smaller downstream distance. The process takes place periodically on either side of the wake to produce laminar vortices at Reynolds numbers up to 350.

When the frequency is varied about the Strouhal frequency f_n the formation region is either expanded or contracted, depending on whether the frequency ratio is less than or greater than unity. These results correspond to the effects of splitter plates, where interference in the vortex formation with a horizontal wake splitter extends the formation region and results in a decrease in the velocity fluctuation on the wake centre-line near $x = l_F$ (Bearman 1965). A decreased formation length for $f > f_n$ was observed by Gerrard (1966) when a vertical wake splitter was placed in the formation region. The velocity fluctuation on the wake axis at formation increases as the vibration frequency is increased from 0·9 to 1·1 f_n for the profiles appearing in figure 4, and the formation region is correspondingly decreased from 2·3 to 1·8 diameters in length. The vibration amplitude was held constant at 30 % of a diameter during these measurements.

These experiments have shown the distance to formation to be a suitable length parameter for the distribution of the velocity fluctuations in the wake; measurements made at a Reynolds number of 144 are plotted in figure 5. The conditions correspond to a decrease in the formation length from 3·2 to 1·7 diameters as the vibration amplitude is increased to half a diameter and all data for the vibrating cylinders were measured in the regime of frequency locking between the vortex shedding and forced vibration. The wake is composed of three regimes: (i) the formation region, in which the shear layers interact and from which vortices are shed; (ii) the stable region, characterized by regular periodicity, an

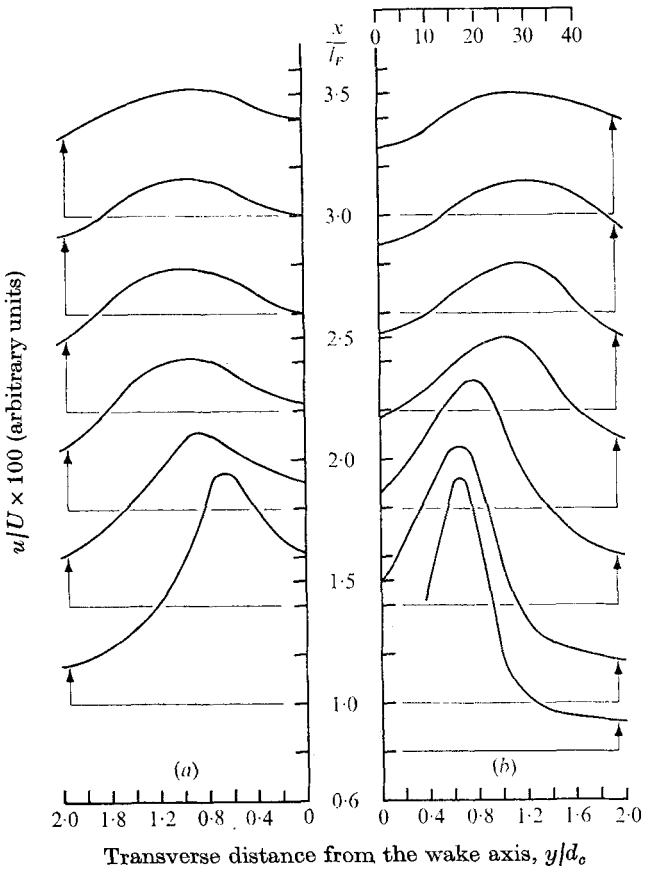

FIGURE 6. Root-mean-square velocity fluctuations in the cylinder wake, at Re = 144, as a function of scaled downstream distance x/l_F and transverse distance y/d_c. The free-stream velocity U was 0·94 m/s and the cylinder was vibrated at $a = 0{\cdot}3d_c$. (*a*) f/f_n = 1·10, (*b*) f/f_n = 0·90.

increase in the transverse vortex spacing and a spreading of the vortex cores, together with a sharp decrease in the amplitude of velocity fluctuations both on and off the wake axis with downstream distance; (iii) the unstable region, generally indicated by a decrease in transverse spacing, the beginning of unstable behaviour, and eventual turbulent breakdown or formation of a new vortex street. Each of these flow regimes has previously beeen observed by Schaefer & Eskinazi (1959) and Taneda (1955) in the classical von Kármán vortex street generated behind the stationary cylinder at Reynolds numbers up to 120–150. The results in figure 5 illustrate the agreement between criteria (i) and (iii) for determining the initial position of the fully formed vortex.

The downstream development of the fluctuating velocity field is shown in figure 6 for frequency ratios 0·9 and 1·10, at a Reynolds number of 144, and the wake development corresponds to the stable region of the flow in $1{\cdot}0l_F < x < 3{\cdot}0l_F$. The maximum off-axis fluctuation at each downstream position in the stable region is less for frequency ratios $f/f_n > 1$ than for $f/f_n < 1$, at the same value

of x/l_F. The results of measurements made on the wake axis indicate an opposite behaviour. The velocity at the end of the formation region is greater for $f/f_n > 1$ than for $f/f_n < 1$, and remains greater as the wake is traversed downstream in the stable region. These results are in contrast to the effects of increased cylinder amplitude alone (Griffin 1971), for which there is an increase in the velocity fluctuation both on and off the wake axis at each downstream distance x/l_F.

5. Vortex phase and spacing

The present experiments included phase measurements in order to determine the effects of frequency and amplitude on the vortex longitudinal spacing l_v, for Reynolds numbers in the transition range. The measurements were made with one anemometer channel and the change in phase angle with downstream distance was measured relative to the cylinder motion signal. This method minimizes probe interference and is quite suitable under the present conditions, since the vibrations correlate the vortex lines parallel to the cylinder axis and the wake is two-dimensional in the stable region. The hot-wire results of Griffin (1971) and the earlier flow visualization observations of Koopmann (1967) show that this is the case. The validity of the method was determined by comparing measurements made with two hot-wire probes; some sample data are included in figure 7.

The relative difference ϕ in figure 7 is between the phase angle measured at a downstream distance x and at the initial position $x = 0$. The phase difference inside the formation region is not representative of the vortex spacing and convection speed as it is farther downstream; in the stable region the vortex spacing function is

$$\frac{l_v}{d_c}\left(\frac{f}{f_n}\right) = 360\frac{\Delta[(x/d_c)\,(f/f_n)]}{\Delta\phi} \tag{1}$$

and is determined from the data for ϕ. The slope of the line was determined from a least-squares fit to the data in the stable region, where the spacing of the vortices is well defined, for three values each of synchronized amplitude and frequency. The relation between ϕ and x becomes

$$\phi = A + B[(x/d)\,(f/f_n)], \tag{2}$$

with $A = -46{\cdot}2° \pm 3{\cdot}8°$ and $B = 65{\cdot}6° \pm 0{\cdot}9°$. The longitudinal spacing results are listed in table 1. There is no change in spacing l_v with cylinder amplitude of motion, but vibration frequencies above and below the natural frequency f_n respectively decrease and increase the longitudinal spacing from its value at the natural frequency. These results are in contrast to the effects of the vibrations on the vortex formation, for which the distance to the initial position of the fully formed vortex is appreciably decreased by greater cylinder amplitude. Both the vortex-formation region and the longitudinal spacing are influenced in the same way by the frequency, resulting in an expansion and contraction of the wake at the lower and higher frequencies.

Some flow-visualization experiments were undertaken in order to complement the hot-wire results just mentioned; representative observations are

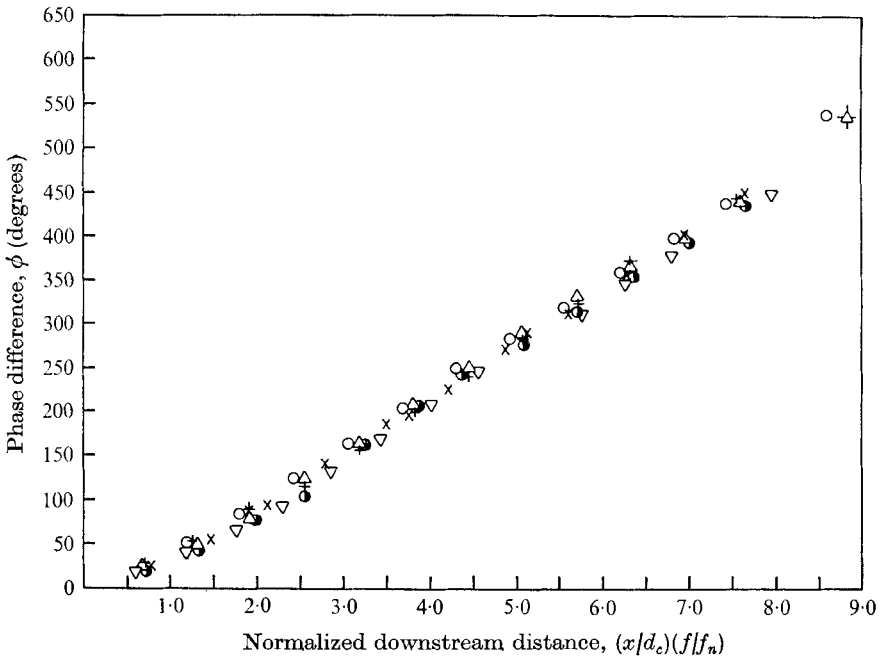

FIGURE 7. Relative vortex phase difference ϕ as a function of the scaled downstream distance $(x/d_c)(f/f_n)$. Re = 144, St = 0·178. The data marked by open circles were measured from two hot wires, all other measurements were made from hot-wire and accelerometer signals.

	+	○	△	◑	▽	×
f/f_n	1·0	1·0	1·0	1·0	0·9	1·1
a/d_c	0·12	0·30	0·30	0·48	0·30	0·30

Frequency ratio f/f_n	Amplitude ratio a/d_c	Vortex spacing l_v/d_c
1·0	0·12	5·4
0·9	0·30	5·9
1·0	0·30	5·4
1·1	0·30	4·9
1·0	0·48	5·4

TABLE 1. Vortex spacing behind a vibrating cylinder. Reynolds number = 144, Strouhal number (natural shedding) = 0·178

displayed in figure 8 (plates 1 and 2). These photographs were taken at a Reynolds number of 220. The model used for the experiments was a six-stranded cable and the general aspects of the flow are quite similar to those for flow around a smooth cylinder (Votaw & Griffin 1971). The photographs were taken with the wake 'frozen' by a strobe and time delay circuit connected to the cylinder motion sensor. For all of the photographs the cylinder is vibrating at an amplitude of 30% of a diameter, and the frequency ratio increases from 0·90 to 1·10 from

figure 8(*a*) to (*c*). Measurements made from the photographs indicate similar effects to those obtained with the hot wire. There appears to be a 25 % decrease in longitudinal spacing as the frequency increases from 37 to 45 Hz, and the results suggest an inverse relation between l_v and f. Such an inverse dependence is also obtained from phase measurements mentioned by Ferguson & Parkinson (1967) in their paper on vortex-excited resonant vibrations. There appears to be little or no change in the vortex convection speed over a substantial range of either free- or forced-vibration parameters as long as the Reynolds number remains unchanged.

The development of the vortex street behind the stationary cylinder at a Reynolds number of 200 is shown in figure 9 (plate 2), and a gradual increase in the transverse spacing with downstream distance appears. A comparison with the photographs in figure 8 shows that the transverse spacing at the two lower vibration frequencies is reduced to such an extent that the street approaches a line of oppositely rotating vortices. Even at the highest frequency ratio, in figure 8(*c*), the transverse spacing behind the vibrating cylinder is decreased (in the region preceding the breakdown of the street) from that of the stationary cylinder wake.

6. Mean flow in the formation and stable regions

The effects of wake synchronization are appreciable not only for the vortex formation and spacing and for the fluctuating velocity distribution, but also for the mean flow in the wake. The velocity profiles in figure 10 show the mean flow development for two cases. These in figure 10(*a*) were obtained in the stationary cylinder wake and those in figure 10(*b*) with the cylinder vibrating at the natural shedding frequency, at 30 % of a diameter. There is a substantial velocity deficit in the formation region behind the stationary cylinder, with the mean velocity on the wake axis reaching 45 % of the free-stream value at the end of the formation region, 3·2 diameters downstream. The end of the formation region is moved upstream by the vibrations to 2·0 diameters behind the cylinder and the mean velocity on the wake axis at this point is increased to 66 % of the free-stream value. The mean flow development after formation is best considered by comparing velocity profiles within the stable region. The profiles at $x = 4{\cdot}4$ diameters for the stationary cylinder and at $x = 2{\cdot}8$ diameters for the vibrating cylinder represent the same relative point in the stable region ($x = 1{\cdot}4\,l_F$) and the mean velocity distributions have reached a corresponding stage of development at this downstream position. A displacement of 3·2 diameters (for the stationary cylinder) marks the initial position of the fully formed vortex, while for the vibrating cylinder this downstream distance is equal to $1{\cdot}6\,l_F$, or well into the stable region. There is little velocity deficit remaining in the wake behind the vibrating cylinder, the mean velocity on the wake axis being equal to 85 % of the free-stream value. The effects of the frequency locking between the vortices and the cylinder are presented in figure 11, where the mean velocity at the end of the formation region is plotted for several values of the vortex-shedding parameter St^*. The increase in St^* is accompanied by a decrease in the size of the

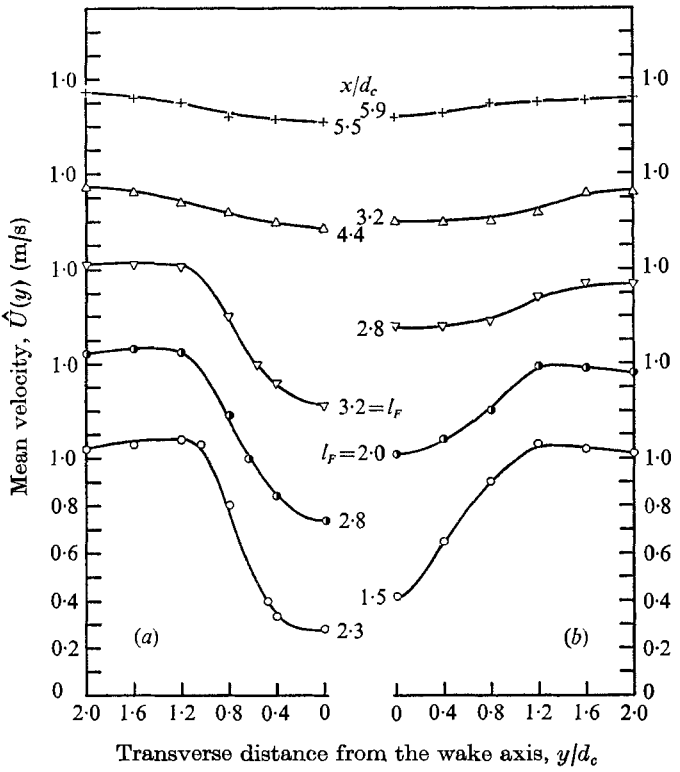

FIGURE 10. Mean velocity in the cylinder wake, at Re = 144, as a function of downstream distance x/d_c. Free-stream velocity = 0·94 m/s. (*a*) Stationary cylinder. (*b*) Vibrating cylinder, f/f_n = 1·0, a/d_c = 0·3.

formation region from 3·2 to 1·7 diameters, and the mean velocity on the wake axis increases from 45% of free-stream value at $St^* = St_n = 0{\cdot}178$ to 72% at $St^* = 0{\cdot}263$.

The velocity-deficit profiles in the near wake offer a means of comparison with related work. The wake decay is expressed in the form

$$\hat{Q}(y) = \frac{\hat{U}_{\max} - \hat{U}(y)}{\hat{U}_{\max} - \hat{U}_{\min}} \tag{3}$$

as a function of the off-axis distance normalized by the wake width $d_{\frac{1}{2}}$, where this parameter denotes the transverse distance marked by the velocity

$$\hat{U}(y)_{y=d_{\frac{1}{2}}} = \tfrac{1}{2}[\hat{U}_{\max} - \hat{U}_{\min}]. \tag{4}$$

This length scale has been used by Kovasznay (1949) and Shaefer & Eskinazi (1959) as a means of estimating the wake width at low Reynolds number behind the stationary cylinder. Results are plotted in figure 12 for several values of St^* (listed in the legend for figure 5) at several downstream displacements in the formation and stable regions of the wake. The exponential character of the wake development is evident when comparison is made with the curve

$$\hat{Q}(y) = e^{-K_1(y/d_{\frac{1}{2}})^m}, \tag{5}$$

$$K_1 = 0{\cdot}742, \quad m = 1{\cdot}870,$$

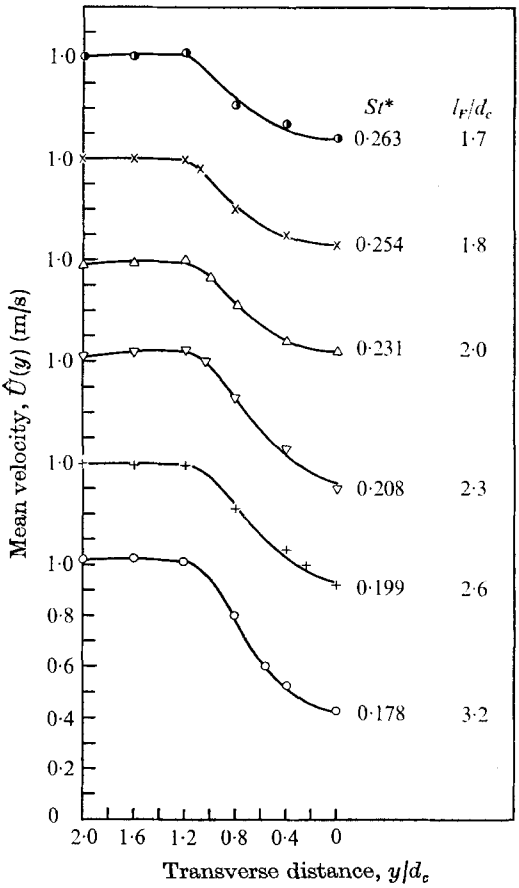

FIGURE 11. Mean velocity at the end of the vortex-formation region, at $Re = 144$, as a function of transverse distance y/d_c. The data are plotted with the shedding number St^* and formation length l_F as parameters. Free-stream velocity = 0·94 m/s.

with the parameters K_1 and m fitted to the data by the method of least squares. Equation (5) was used by Shaefer & Eskinazi and the agreement between the present data and this equation is comparable to that of their stationary-cylinder results at $Re = 62$, for which they found that $K_1 = 0{\cdot}693$, $m = 2{\cdot}0$ yielded a satisfactory description of the velocity-deficit profiles.

7. The unstable region of the wake

The wake of the vibrating cylinder at each Reynolds number up to 350 is composed of the three classical flow regimes: the formation, stable and unstable regions, as shown in figure 5. Such behaviour is evident at all Reynolds numbers in our experiments and is accompanied by a decrease in the downstream position to which the stable region extends. The ratio of the stable- and formation-region lengths is plotted in figure 13. The ratio l_s/l_F decreases from 3·2 at $Re = 120$ to 1·3 at $Re = 350$ and this is accompanied by a decrease in the maximum down-

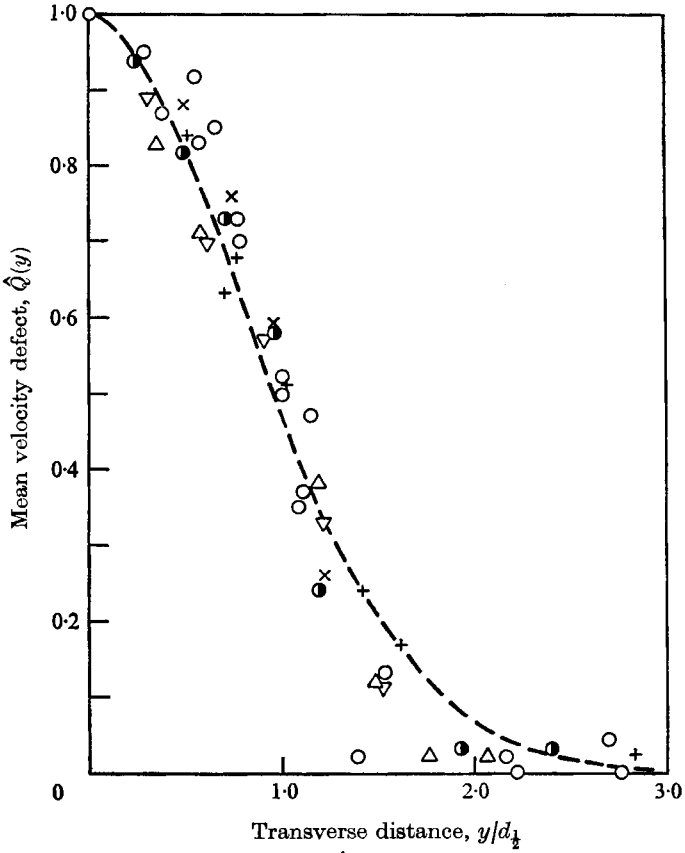

FIGURE 12. Mean velocity defect $\hat{Q}(y)$ as a function of normalized transverse distance $(y/d_{\frac{1}{2}})$ at $Re = 144$, $St_n = 0{\cdot}178$. – – –, equation (5).

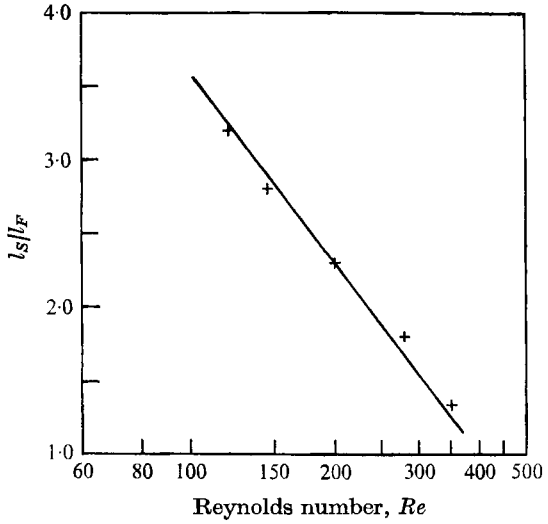

FIGURE 13. The ratio of the stable-region length l_S and formation-region length l_F as a function of Reynolds number in the regime of laminar-stable shedding.

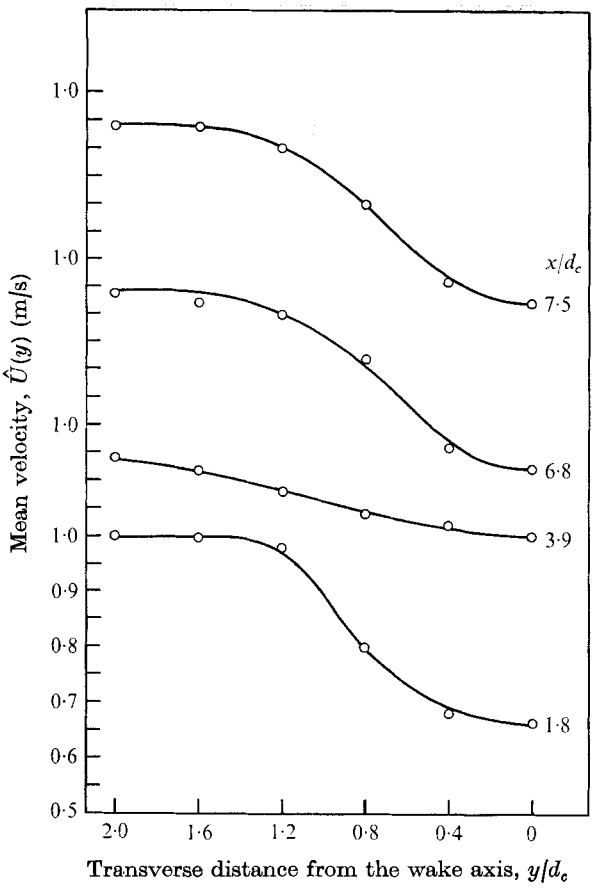

FIGURE 14. Mean velocity profiles recorded in the wake of a vibrating cylinder at a Reynolds number of 144, for a vibration of 110% of the natural shedding frequency and an amplitude of 30% of a diameter. Free-stream velocity = 0·94 m/s.

stream wake width $d_{\frac{1}{2}}$ from 1·2 to 0·6 d_c over the same Reynolds number range. The beginning of the unstable region is defined in this and earlier work (Griffin 1971) to be the downstream distance at which the regions of maximum off-axis fluctuation begin to converge toward the wake axis. Some representative results are listed in table 2.

There are several characteristics of the unstable region that have been observed in studies of the von Kármán vortex street behind stationary cylinders. Taneda (1955) reported that the unstable region precedes the turbulent breakdown of the wake or the formation of a new vortex street of larger geometry for Reynolds numbers up to 150. Schaefer & Eskinazi (1959) report the decrease in spacing at large downstream distances, and Zdravkovich (1967) observed the breakdown and decrease in spacing together with upstream movement of the transition as the Reynolds number increased from 100 to 300. More recently, Durgin & Karlsson (1971), using a hot wire to study vortex street breakdown, observed the reappearance of a substantial velocity deficit a short distance downstream from a circular cylinder behind which the vortex street was formed in the

Reynolds number Re	Frequency ratio f/f_n	Amplitude of vibration a/d_c	Stable-region length l_s/d_c	l_s/l_F
144	1·0	0·12	7·3	2·8
	0·9	0·30	6·4	
	1·0	0·30	5·6	
	1·1	0·30	5·0	
200	1·0	0·12	5·3	2·2
	0·89	0·30	5·1	
	1·0	0·30	4·2	
	1·11	0·30	3·8	
280	1·0	0·12	4·0	1·8
	1·0	0·30	3·1	

TABLE 2. The effect of Reynolds number and frequency-locked vibrations on the stable region of vortex shedding

usual manner and later subjected to deceleration. Goldstein (1938) gave a theory explaining these characteristics in an early study of the vortex street.

The mean velocity profiles in figure 10, measured in the formation and stable regions, follow the usual behaviour of the von Kármán street, with the velocity deficit disappearing as the wake development proceeds (cf. Schaefer & Eskinazi 1959). The vortex street in figure 8(*c*) (plate 2) shows evidence of breaking up downstream at a distance that corresponds to the unstable region of the wake. This vortex wake breakdown has the same appearance as that observed by Zdravkovich in his flow-visualization experiments, except that in the present experiment the appearance of instability is dependent on the vibratory parameters. Koopmann (1967) also observed that the region of instability moved upstream as the vibration frequency was increased within the frequency-locked regime at $Re = 200$. The vortex street in figure 8(*c*) also shows evidence of distortion and elongation of the vortex cores in the unstable region, both of which concur with Zdravkovich's stationary cylinder wake observations.

Several mean velocity profiles were recorded at $Re = 144$, for cylinder motion of amplitude 30% of a diameter and 110% of the Strouhal frequency and are plotted in figure 14. The stable region extends five diameters downstream under these vibratory conditions, which are similar to those of figure 8(*c*). A substantial mean velocity deficit reappears in the unstable region of the wake at 6·8 and 7·5 diameters downstream. The possibility that this behaviour results from inaccuracies of measurement can be discounted, since particular care was taken in the linearization of the hot-wire output. This reappearance of the wake deficit agrees with the observations of Durgin & Karlsson (1971); the Reynolds number in their experiment was about 170. The behaviour observed in the present experiments for the wakes of vibrating cylinders shares many basic characteristics with previous observations of the von Kármán vortex street behind stationary cylinders. It is possible to conclude that the unstable regions of the wake retains much of this basic character, including the reappearance of a mean velocity deficit, distortion of the vortex cores and irregular behaviour of the street. The

extent of the formation and stable regions and the initiation of the unstable region are dependent on the Reynolds number, the vibration frequency and the vibration amplitude in the regime where the vortex shedding and vibration frequencies lock together to control the wake. There is a noticeable increase in the amplitude of the velocity fluctuations in the vibrating cylinder wake, as is shown by the present results and those previously reported (Griffin 1971). The stable von Kármán vortex street has been observed only below Reynolds numbers between 120–150 behind a stationary cylinder, whereas it may occur for a Reynolds number of up to 350 behind a vibrating cylinder.

8. Summary and conclusions

Throughout the course of this experimental programme we have attempted to study systematically the effects of forced transverse vibrations on the vortex wake behind a vibrating cylinder. All results were obtained for the flow regime where the vibration and vortex frequencies lock together when a bluff body is vibrated in a uniform crossflow.

The vortex formation is controlled by the forced vibrations, with the distance to the initial position of the fully developed vortex being determined by a shedding parameter St^* related to the Strouhal number, the frequency and the amplitude of the vibrations. Vibrations at the Strouhal frequency of half a diameter reduce the formation length by 50 % at a Reynolds number of 144. The formation length is a suitable scaling parameter for the downstream distribution of velocity fluctuations in the wake at each Reynolds number up to 350.

The wake of the vibrating cylinder can be divided into the three classical flow regimes of the laminar Kármán vortex street: the formation, stable and unstable regions. The length of the stable region is simply dependent on the formation length at each Reynolds number for which the wake remains laminer after formation. The stable region has been observed to occur only up to Reynolds numbers of 120–150 for the stationary cylinder, whereas it is observed for Reynolds numbers to 350 when the cylinder is vibrated in the frequency-locked regime. The longitudinal spacing of the vortices in the stable region is inversely dependent on the vibration frequency, but is unaffected by the amplitude of the vibrations so long as the frequency remains unchanged.

The general character of the vortex street breakdown in the unstable region behind the vibrating cylinder corresponds to previous observations of wake instability and turbulent breakdown in the von Kármán street behind stationary cylinders at lower Reynolds numbers. The reappearance of a large mean velocity deficit, distortion of the laminar vortices and decreased transverse spacing have been observed.

The authors wish to acknowledge the Ocean Technology and Acoustics Divisions of the Naval Research Laboratory for their support of this work. A particular note of thanks is due to J. Otto for his work with our photographic negatives.

REFERENCES

BEARMAN, P. W. 1965 *J. Fluid Mech.* **21**, 241–255.

BERGER, E. W. 1964 *Jahr. Wiss. Ges. L. & R.* Berlin.

BERGER, E. W. 1967 *Phys. Fluids*, **10**, S 191–S 193.

BISHOP, R. E. D. & HASSAN, A. Y. 1964 *Proc. Roy. Soc.* A **277**, 32–75.

BLOOR, M. S. 1964 *J. Fluid Mech.* **19**, 290–304.

BLOOR, M. S. & GERRARD, J. H. 1966 *Proc. Roy. Soc.* A **294**, 319–342.

DURGIN, W. & KARLSSON, S. 1971 *J. Fluid Mech.* **48**, 507–527.

FERGUSON, N. & PARKINSON, G. 1967 *Trans. A.S.M.E. J. Eng. Industr.* **89**, 831–838.

GERRARD, J. H. 1966 *J. Fluid Mech.* **25**, 401–143.

GOLDSTEIN, S. 1938 *Modern Developments in Fluid Mechanics*, vol. 2. Oxford University Press.

GRIFFIN, O. M. 1971 *J. Appl. Mech.* **38**, 729–738.

GRIFFIN, O. M. 1972 *Trans. A.S.M.E., J. Eng. Indust.* **94**, 539–547. (See also *A.S.M.E. Vibrations Conference Preprint*, 71-Vibr-25.)

KOOPMAN, G. H. 1967 *J. Fluid Mech.* **28**, 501–512.

KOVASZNAY, L. S. G. 1949 *Proc. Roy. Soc.* A **198**, 175–190.

MAIR, W. A. & MAULL, D. J. 1971 *J. Fluid Mech.* **45**, 209–224.

MEI, V. C. & CURRIE, I. G. 1969 *Phys. Fluids*, **12**, 2248–2254.

ROSHKO, A. 1954*a* *N.A.C.A. Rep.* no. 1191.

ROSHKO, A. 1954*b* *N.A.C.A. Tech. Note*, no. 3169.

SCHAEFER, J. W. & ESKINAZI, S. 1959 *J. Fluid Mech.* **6**, 241–260.

TANEDA, S. 1955 *Rep. Res. Inst. Appl. Mech.* **4**, 29–40.

TOEBES, G. H. 1968 *Trans. A.S.M.E. J. Basic Eng.* **91**, 493–505.

TOEBES, G. H. & RAMAMURTHY, A. S. 1967 *Proc. A.S.C.E. J. Eng. Mech.* **93** (EMG), 1–20.

VOTAW, C. W. & GRIFFIN, O. M. 1971 *Trans. A.S.M.E. J. Basic. Eng.* **93**, 457–461.

ZDRAVKOVICH, M. M. 1967 *J. Roy. Aero. Soc.* **71**, 866–867.

ZDRAVKOVICH, M. M. 1968 *J. Fluid Mech.* **32**, 339–351.

(*a*)

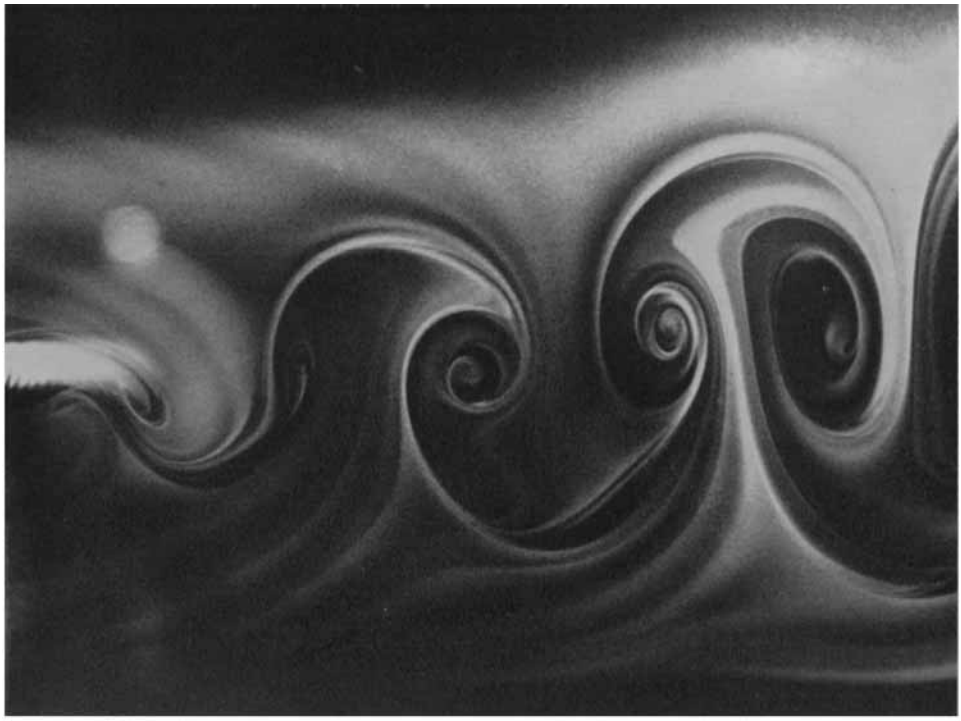

(*b*)

FIGURE 8. Vortex shedding from a vibrating six-stranded cable at a Reynolds number of 220. The vibration amplitude was held constant at $a = 0{\cdot}3d_c$. (*a*) $f = 37$ Hz, $f/f_n = 0{\cdot}9$. (*b*) $f = 41$ Hz, $f/f_n = 1{\cdot}0$. (*c*) $f = 45$ Hz, $f/f_n = 1{\cdot}1$.

FIGURE 8*c*. For legend see previous page.

FIGURE 9. Vortex shedding from a stationary six-stranded cable at a Reynolds number of 220. Shedding frequency f_n = 41 Hz.